# ACOUSTOELASTICITY USING LONGITUDINAL WAVES

# FOR RESIDUAL STRESS EVALUATION

J.J. Dike and G.C. Johnson
Department of Mechanical Engineering
University of California
Berkeley, CA 94720

E.C. Flower
Lawrence Livermore National Laboratory
Livermore, CA 94550

## INTRODUCTION

Residual stresses play an important role in the behavior of structures during machining and under load . Knowledge of these residual stress states allows better and more efficient use of the structures, as well as more accurate predictions of their behavior. In this paper, a new method for nondestructively evaluating complete states of plane residual stress is presented. The basic analytical and experimental procedures are reviewed, and results of estimated residual stresses are compared with numerical predictions.

Several methods are available for determining residual stresses. Nondestructive techniques include x-ray and neutron diffraction studies that measure residual strains through determination of crystal lattice spacing. Here we examine the application of a nondestructive technique called acoustoelasticity which employs ultrasonic waves in the evaluation of residual stress states.

The acoustoelastic technique is based on the fact that the speed at which a wave propagates through a solid body is affected by the state of stress in the body. There are several stress evaluation techniques which make use of the acoustoelastic effect, all of which rely on an assumption of plane stress. The most common is the birefringence technique [1-3] which uses two shear waves propagating normal to the plane of stress, polarized in the principal stress directions. In general, the speeds of the two waves are different, with the difference in the speeds related to the difference in the principal stresses. If the material in question is initially isotropic, the wave speed difference is proportional to the stress difference. Usually, however, materials are not initially isotropic and the relation between velocity change and stress is somewhat more complicated.

Another acoustoelastic technique which is receiving considerable attention uses two shear horizontal (SH) waves propagating along the principal stress directions with their polarizations in the other principal stress directions [4-6]. These waves travel at different

speeds, and the difference in the speeds is directly related to the difference in principal stresses. Knowledge of elastic and acoustoelastic constants is not required and the difficulties associated with initial anisotropy are less severe than in the birefringence technique.

The technique considered here uses longitudinal waves propagating normal to the plane of stress. Through use of a new method for treating the measurements, the entire residual stress state can be determined [7]. In this case, the speed of propagation through an initially isotropic material is proportional to the sum of the principal stresses. The constant of proportionality is usually determined by performing a uniaxial tension test in which the velocity change from the initial unstressed condition is determined at various stress levels. The slope of the stress-velocity curve is the acoustoelastic constant. The maximum change in velocity for metals is generally less than one percent at yield.

The focus of our work on longitudinal waves stems from the ease with which measurements may be made over the entire surface of a planar sample and the spatial resolution which can be achieved in such a scan. The birefringence and SH wave methods are less attractive from this point of view. Piezoelectric transducers for shear waves require viscous couplants or contact with the specimen to launch the waves. This fact, along with the relatively large region illuminated by the transducers, limits the number of measurements that are taken over the specimen surface. Electromagnetic acoustic transducers (EMATs) currently employed for most of the SH wave work do not require a couplant or contact with the specimen, but current EMAT designs do not permit spatial resolution approaching that achieved with longitudinal waves.

## THEORETICAL BASIS

We begin with the assumptions that the material is in a plane state of residual stress, and that it is initially homogeneous. The acoustoelastic response is assumed to be isotropic (the same velocity change for loading in any direction in the plane), but the material is not assumed to be elastically isotropic. Under these conditions, the change in longitudinal wave speed $\Delta V$ relative to the speed $V_o$ in the unstressed state is proportional to the sum of the principal stresses [2]

$$\frac{\Delta V}{V_o} = P(\sigma_{xx} + \sigma_{yy}) = P\,\sigma_{\alpha\alpha}, \tag{1}$$

where P is the velocity - acoustoelastic constant, $\sigma_{xx}$ and $\sigma_{yy}$ are the cartesian components of normal stress, and $\sigma_{\alpha\alpha}$ is the sum of the in-plane stresses (the first invariant of the stress tensor).

The equilibrium equations for the state of plane stress with no body forces are

$$\begin{aligned} \sigma_{xx,x} + \sigma_{xy,y} &= 0, \\ \sigma_{xy,x} + \sigma_{yy,y} &= 0. \end{aligned} \tag{2}$$

Differentiating $(2)_1$ with respect to y and $(2)_2$ with respect to x and adding gives

$$\nabla^2\sigma_{xy} = -\sigma_{\alpha\alpha,xy}. \tag{3}$$

Equation (3) is a Poisson's equation for the shear stress $\sigma_{xy}$ in terms of a derivative of the invariant $\sigma_{\alpha\alpha}$. We are able to determine the right-hand side of Eq. (3) from measurements of $\Delta V/Vo$ and knowledge of the acoustoelastic constant P, as in equation (1).

In order for Eq. (3) to be associated with a well-posed problem, the boundary conditions must be considered. At the boundary, the normal stresses may be written in terms of the normal and tangential components of stress, $\sigma_{nn}$ and $\sigma_{tt}$, respectively, while the shear stress is $\sigma_{nt}$. Because we consider only residual stresses, the boundary is taken to be traction free and so $\sigma_{nn} = \sigma_{nt} = 0$. Thus, $\sigma_{\alpha\alpha} = \sigma_{tt} + \sigma_{nn} = \sigma_{tt}$. Since we assume that we are able to determine $\sigma_{\alpha\alpha}$ everywhere from velocity variation measurements, we are able to calculate the shear stress component in cartesian coordinates, $\sigma_{xy}$, along the boundary from knowledge of the outward unit normal.

Once the Poisson's equation (3) has been solved, the equilibrium equations (2) may be integrated to obtain the normal stress components $\sigma_{xx}$ and $\sigma_{yy}$. Thus the complete residual stress state may be estimated from knowledge of $\sigma_{\alpha\alpha}$ at each point of the body and the outward unit normal.

In performing the experiments associated with this technique, there are two different types of velocity variations which are important. We refer to these as configurational variations and spatial variations. Associated with these, we make the following definitions:

$\Delta V/Vo$ is the configurational velocity change. It is the relative velocity change between the final and initial configurations, at the same point.

$\delta V/V$ is the spatial velocity variation. It is the relative velocity difference between two points in the final configuration.

In defining these quantities mathematically, we consider the longitudinal wave speeds at two material points, x and $x_r$, in both the initial and final configurations. We will refer to $x_r$ as the reference point. Since the material is initially homogeneous, we have that $V_i(x) = V_i(x_r) = V_o$. The wave speeds $V_f(x)$ and $V_f(x_r)$ in the final configuration are in general different. The configurational change for the point x is expressed as

$$\frac{\Delta V}{V_o} = \frac{V_f(x) - V_o}{V_o} \tag{4}$$

while the spatial variation is expressed as

$$\frac{\delta V}{V} = \frac{V_f(x) - V_f(x_r)}{V_f(x_r)} . \tag{5}$$

Unfortunately, velocity is not a directly measurable quantity. The velocity variations we "measure" are actually calculated from measurements of variations of the time-of-flight for the wave and the thickness of the specimen. Thus, two types of scans are used: one to provide the spatial variation in thickness d(x) and one to provide the spatial variation in time-of-flight T(x). The system used to make the thickness scans has been described by Fisher and Johnson[8]. It uses two colinear transducers separated by a distance L with the specimen mounted between them. The measurand in this system is the frequency of the waves

required to maintain a specific phase condition between the first echoes arriving at the transducers. The relation between the thickness variation and the frequency variation is

$$\frac{\delta d}{d}\left[1 + \frac{\delta f_d}{f_d}\right] - \frac{L - d_r}{d_r}\,\frac{\delta f_d}{f_d} = 0, \tag{6}$$

where $d_r$ is the the thickness at the reference point $x_r$, $f_d$ denotes the frequency associated with the thickness scan, and $\delta$ again indicates spatial variation in the appropriate quantity. We note that this expression is exact, whereas the expression given by Fisher and Johnson [8] is a linearization of Eq. (6).

The time-of-flight scan requires only one transducer. It also evaluates the frequency at which a particular phase condition exists between two echoes - one which has passed through the sample, and one which has merely reflected off the face of the sample. In this case, the measured frequency is denoted $f_T$. The spatial velocity variation is then computed through the relation

$$\frac{\delta V}{V} = \frac{\delta d}{d} + \frac{\delta f_T}{f_T} + \frac{\delta d}{d}\,\frac{\delta f_T}{f_T} \tag{7}$$

Equation (7) is also an exact expression. The second-order term is included because the first and second terms on the right-hand side of Eq. (8) are often of nearly equal magnitudes and of opposite signs. Their sum is therefore small, and the second-order term may be significant, particularly in materials with small acoustoelastic constants.

## NUMERICAL PROCEDURES

Measurements cannot be made along the boundary due to scattering of the transducer beams. Therefore, data from the interior of the region is extrapolated to the boundaries using a simple extrapolation algorithm.

Once the two scans have been performed and the data extrapolated to obtain spatial variations for the entire sample, the configurational velocity change at each point must be computed so that we can obtain the estimate of $\sigma_{\alpha\alpha}$ from Eq. (1). To evaluate this configurational change data, let us expand Eq. (5) as

$$\frac{\delta V}{V} = \frac{V_f(x) - V_o}{V_f(x_r)} - \frac{V_f(x_r) - V_o}{V_f(x_r)} = \frac{V_o}{V_f(x_r)}\left[\frac{\Delta V}{V_o} - C\right] \tag{8}$$

where C is the configurational velocity change at the reference point. Since the velocity changes are small (less than 1%), we approximate the desired relation as

$$\frac{\Delta V}{V_o} = \frac{\delta V}{V} + C\ . \tag{9}$$

Our task now is to determine C.

Recall that the stress state considered is residual and so must be self-equilibrating. It then follows that the integral of the sum

$\sigma_{\alpha\alpha}$ over the entire surface area $\Sigma$ must vanish. Thus, on integrating Eq. (9) over the region we find that

$$C = -\frac{1}{\Sigma}\int \frac{\delta V}{V}\, d\Sigma \quad . \tag{10}$$

The stresses $\sigma_{\alpha\alpha}$ may then be evaluated by

$$\sigma_{\alpha\alpha} = \frac{1}{P}\left[\frac{\delta V}{V} + C\right] . \tag{11}$$

## EXPERIMENTAL RESULTS

An annulus of 6061-T6 aluminum, with nominal thickness of 12.7 mm, inside diameter of 38.1 mm, and outside diameter of 63.5 mm, was loaded in diametral compression until permanently deformed and then completely unloaded. Loading was performed using ball-in-socket compression platens acting on flat regions which had been machined on the top and bottom of the annulus. Two 10 MHz, focussed transducers were used to scan one quadrant of the specimen over a 2.54 mm radial, 10 degree circumferential grid. Experimentally determined stress contours were compared with those estimated by the NIKE2D finite element code [9].

The stresses were determined through use of the finite difference scheme described in [7]. As described in the previous section, the measured frequencies were first used to compute the configurational velocity change and associated stress sum $\sigma_{\alpha\alpha}$ at each scan point through Eqs. (6) - (11). The Poisson's equation for $\sigma_{xy}$ was then solved numerically in polar coordinates, and finally, the normal stresses were obtained by integrating the equilibrium equations.

The residual pressure $(-\sigma_{\alpha\alpha}/3)$ contours shown in Fig. 1 indicate generally good agreement between the two solutions. Note in particular the results of the two approaches for the zero contour (D). While the experimental contour is somewhat noisier than the numerical contour, the overall agreement indicates that the method for evaluating the constant C, and so the sum of stresses $\sigma_{\alpha\alpha}$, is valid. The fact that the experimental contours are noisier than the numerical contours is to be expected due to the intrinsic uncertainty in the measurements. This is especially noticeable in the essentially stress free regions of the annulus. We also note that the contours generally have the correct shape and are properly located spatially. Two regions that deserve mention because of their lack of agreement, however, are the top near the loading flat and the outside edge near the side. In the case of the top, the extrapolation and subsequent evaluation of the constant C did not account for the material removed in machining the loading flat. Thus, the compressive stress in this region at the top is considerably larger than in the numerical case. At the right-hand edge of the experimental plot, there is a region of relatively large compressive stress. This appears to be due to errors in a small number of data points which are exaggerated in the extrapolation process.

Figure 2 presents the experimental and numerical estimates of the shear stress $\sigma_{xy}$. Again, the zero-stress contour (E) has the same basic pattern throughout the region and is noisier in the experimental plot. The regions of positive and negative shear are in uniform

agreement, though there are again certain regions within which the magnitudes are somewhat different. Under the flat at the top, for example, the experimental contours accurately denote the stress concentration at the edge of the flat, but overpredict the magnitude of the shear stress at this point. Similarly, the region at the right-hand side where the noisy data in the pressure was observed has a peak in the shear which is missing in the numerical estimate.

Figure 3 presents contours for the normal stress $\sigma_{xx}$ - the hoop stress along the axis of loading. The region in which this stress component is small is accurately detected and, as in the previous plots, the zero-stress contours agree reasonably well. The regions of tension

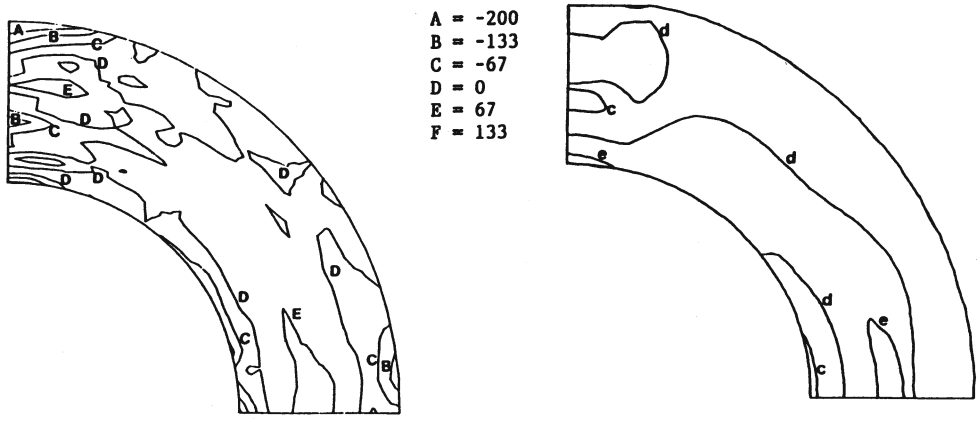


Figure 1. Contours of residual pressure ($-\sigma_{\alpha\alpha}/3$) for 6061-T6 aluminum annulus: experimental results (left) and numerical results (right). Contour levels given in MPa.

and compression are in spatial agreement, though the magnitudes of the experimental estimates are higher than those of the numerical estimates. This is especially true at the boundaries where the extrapolation plays such a dominant role.

Extrapolation tends to be an inherently inaccurate process, and as noted above, can cause substantial difficulties at the boundaries. It was found that while various extrapolation procedures yielded large differences in the values of stresses at the boundary, the interior values were affected very little. The larger the ratio of area where measured data is available to that where extrapolated values must be used, the better the results of this method can be expected to be.

ACKNOWLEDGEMENTS

This work was supported by the Lawrence Livermore National Laboratory through the Engineering Research and Development Program and by IBM Almaden Research Center.

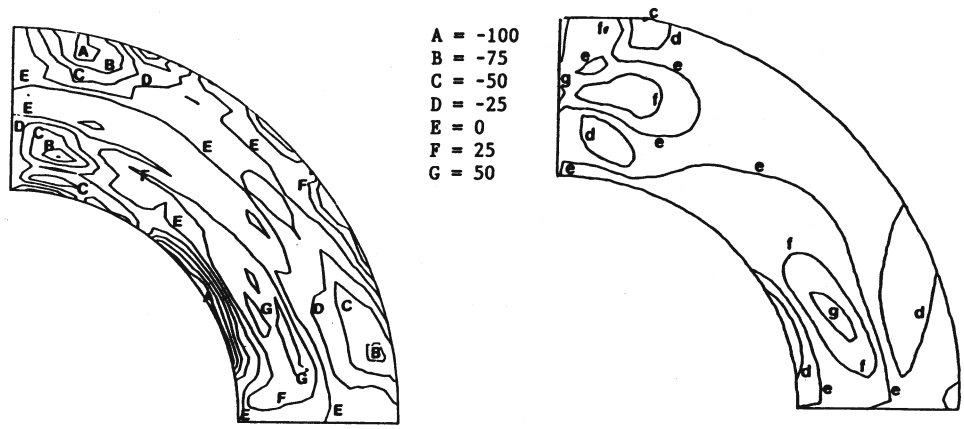


Figure 2. Contours of residual shear stress $\sigma_{xy}$ for 6061-T6 aluminum annulus: experimental results (left) and numerical results (right). Contour levels given in MPa.

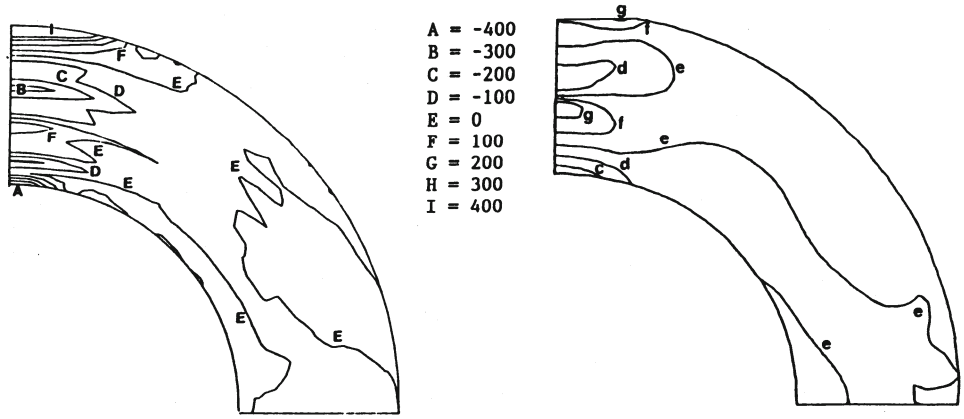


Figure 3. Contours of residual normal stress $\sigma_{xx}$ for 6061-T6 aluminum annulus: experimental results (left) and numerical results (right). Contour levels given in MPa.

REFERENCES


1. N.N Hsu, Exp. Mech. 14, 169 (1974).
2. H. Fukuoka, H. Toda, and N. Naka, Exp. Mech., 23, 120 (1983).
3. Y.-H. Pao, W. Sachse, and H. Fukuoka, in Physical Acoustics, edited by W.P. Mason and R.N. Thurston (Academic Press, New York, 1984), Vol. XVII, Chap. 2.
4. R.B. King and C.M. Fortunko, J. Appl. Phys., 54, 3027 (1983).
5. R.B. Thompson, S.S. Lee, and J.F. Smith, J. Acoust. Soc. Am., 80, 921 (1986).
6. C.-S. Man and W.Y. Lu, J. Elasticity, 17, 159 (1987).
7. G.C. Johnson and J.J. Dike, in Review of Progress in Quantitative NDE, edited by D.O. Thompson and D.E. Chimenti (Plenum Press, New York, 1988), Vol. 7B, pp. 1391-1398.
8. M.J. Fisher and G.C Johnson, in Review of Progress in Quantitative NDE, edited by D.O. Thompson and D.E. Chimenti (Plenum Press, New York, 1984), Vol. 3B, pp. 1119-1128.
9. J.O. Hallquist, NIKE2D - A Vectorized Implicit, Finite Deformation, Finite Element Code for Analyzing the Stat and Dynamic Response of 2-D Solids with Interactive Rezoning and Graphics, Lawrence Livermore National Laboratory UCID No. 19677, Livermore, CA (1986).